OUKA
Osaka University Knowledge Archive

Title	Formation and Structure of Crystalline Phase TiB_2 Films by Ion Beam Assisted Deposition(Physics, Process, Instrument & Measurements)
Author(s)	Wang, Yu; Setsuhara, Yuichi; Miyake, Shoji
Citation	Transactions of JWRI. 1994, 23(1), p. 7-11
Version Type	VoR
URL	https://doi.org/10.18910/9096
rights	
Note	

Osaka University Knowledge Archive : OUKA

https://ir.library.osaka-u.ac.jp/

Osaka University

Formation and Structure of Crystalline Phase TiB_2 Films by Ion Beam Assisted Deposition†

Yu WANG*, Yuichi SETSUHARA** and Shoji MIYAKE***

Abstract

Ion beam assisted deposition (IBAD) technique was used to fabricate TiB_2 films using argon ion bombardment during the deposition of TiB_2 by electron beam evaporation. The formation and dependence of crystalline structure and microhardness of TiB_2 films on the energy of Ar^+ were studied by changing the Ar^+ energy from 2 to 20 keV while keeping the transport ratio constant. Ruthurford backscattering spectroscopy indicated that the film composition had stoichiometry of TiB_2. The as-deposited film, prepared without Ar^+ bombardment, was found to be non-crystalline (or lack of long range order) and had relatively low microhardness. The films deposited with simultaneous Ar^+ bombardment were crystalline and had very high microhardness over 3000 kgf/mm^2 when the energy of Ar^+ was larger than 5 keV.

KEY WORDS: (Ion Beam Assisted Deposition) (Hard Coatings) (Titanium Borides) (TiB_2)

1. Introduction

With the increasing demand for the improved performance of engineering components, surface modification using films of various superior materials has become necessary to enhance the wear and corrosion resistance of conventional materials[1] Among all the possible selections of such materials, transition metal (TM) boride, especially TiB_2, has been proved a good candidate for this purpose, because of its high hardness, high melting points, and good inertness to chemical and melting metal erosion[2,3]. In addition, TiB_2 film, because of its high electrical conductivity and stability to thermal and electrical migrations[4,5], can be used in microelectronic devices as diffusion barriers between metallic contacts and the silicon substrate. Thorough control over the structure and properties of TiB_2 films during the film forming process is demanded. In that sense, Ion Beam Assisted Deposition (IBAD) is considered to be a superior method to synthesize TiB_2 films over many other film forming techniques currently in use, such as chemical vapor deposition (CVD)[6], magnetron sputtering[7], rf sputtering[8] and plasma spray coating[9].

IBAD, employing simultaneous ion beam bombardment during the film deposition, can introduce film forming species and transfer certain amounts of energies into the growing films. So IBAD is characterized by its ability to synthesize hardmelting compound films at a relatively low substrate temperature, and IBAD can easily control the structure, composition and phase formation in the growing films. It had been extensively used to synthesize both metallic and ceramic films. IBAD is also distinguished by its ability to form an atomic intermixed layer between the film and the substrate, which can greatly enhance the adhesion of the film. This is particularly desirable to synthesize films of ultra hard materials, such as metal nitride, carbide and boride, whose brittleness has limited their wide use as wear and corrosion resistant coatings. Recently, J.P. Rivièe et al.[10,11] have reported on the synthesis of TiB_2 films using dynamic ion mixing with 320 keV Ar and Xe ions. In their work, crystallized films with a B/Ti atomic ratio of 1.4 have been obtained.

In the present work, TiB_2 films were prepared using the electron beam evaporation with the simultaneous bombardment of medium energy (2 to 20 keV) argon ions. IBAD using medium energy ions is more suitable for the actual application because it produces less damage to the substrate and is very easy and relatively inexpensive to operate. The dependence of the film structure as well as mechanical properties on the energy of Ar^+ has been studied systematically.

† Received on July 11, 1994

* Research Associate, Space Science and Application Research Center, Beijing China

** Research Associate

*** Professor

Transactions of JWRI is published by Welding Research Institute, Osaka University, Ibaraki, Osaka 567, Japan

2.Experimental Procedure

TiB_2 films were prepared in an IBAD apparatus[12] equipped with an electron beam evaporator and an electron-cyclotron-resonance (ECR) ion source with an ion-beam energy of 2 to 20 keV. The chamber was first evacuated to a base pressure of about 2.7×10^{-4} Pa by a cryopump and a turbomolecular pump. Before the film preparation, the Si(111) substrate was cleaned by sputtering with a 2 keV Ar^+ beam to eliminate surface contamination. TiB_2 films were deposited by evaporating TiB_2 material in a BN crucible, with electron beam heating. The deposition rate of the film was monitored by using an INFICON-XTC quartz crystal oscillator. Simultaneous Ar ion bombardment was employed during the deposition of TiB_2 films. The working pressure during the IBAD process was about 2.9×10^{-3} Pa. Various films were prepared by changing the energy of Ar^+ ions from 2 to 20 keV with the Ar^+ ion to TiB_2 molecule transport ratio (represented by Ar^+/Ti) kept nearly constant at 0.4. The incidence angle of the Ar^+ beam was 45° to the normal of the substrate. The substrate temperature was controlled to be less than 200 °C by a water cooling system. The total thickness of all films was about 5000 Å as monitored by the quartz crystal oscillator. An inter-mixed layer was introduced with the initial 1000 Å of all films deposited with 10 keV Ar^+ bombardment, in order to enhance the adhesion of the film to the substrate.

The chemical composition of the films was measured by Ruthurford backscattering spectrometry (RBS) using 2 MeV ^4He ions with a back-scattering angle of 165°. Both standard θ–2θ and glancing angle X-ray diffraction (XRD), using Cu Kα radiation, were used for the characterization of the crystalline structure of TiB_2 films. The Vickers microhardness of the films was also measured.

3. Results and Discussions

3.1 The film composition

The film composition was measured by RBS for both as-deposited and Ar^+ bombarded films (See Fig.1). Both films had almost the same B to Ti atomic ratio of about 2:1, which corresponds to the stoichiometric composition of TiB_2. For the as-deposited film, a considerable amount (about 21%) of oxygen contamination was observed. No oxygen contamination could be detected in the film deposited with Ar^+ bombardment, while a little amount of Ar atoms was observed in the film.

During the film deposition, the TiB_2 material, heated by the electron beam, seemed to be evaporated directly

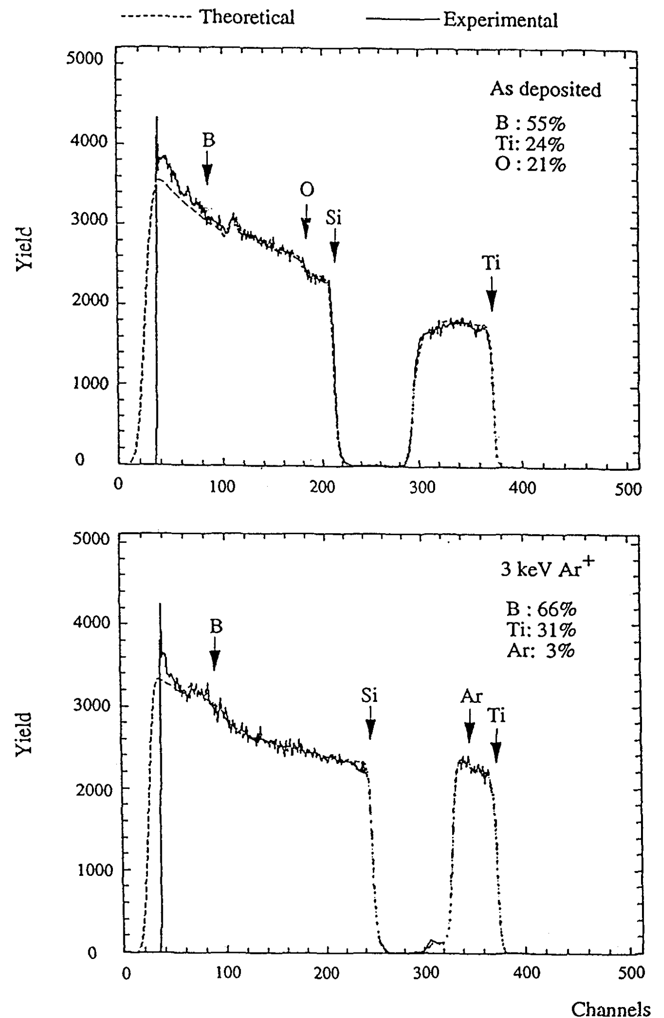

Fig.1 The Ruthurford backscattering spectra of IBAD TiB_2 films

from the solid state without being melted first. So the composition segregation, which usually took place for the evaporation of most of metal alloys and compounds, did not take place in this case. That was why the films prepared in our work had nearly the same composition as that of the evaporating material. In this sense, the electron beam evaporation has the advantage over the sputtering deposition, in which films with the B/Ti atomic ratio of 1.4 have been obtained[11]. The oxygen contamination in the as-deposited film was considered to be due to the residual oxygen in the experimental chamber. However, the oxygen contamination in the IBAD films is considerably reduced by the bombardment with Ar ions through the selective sputtering of oxygen atoms out of the growing film.

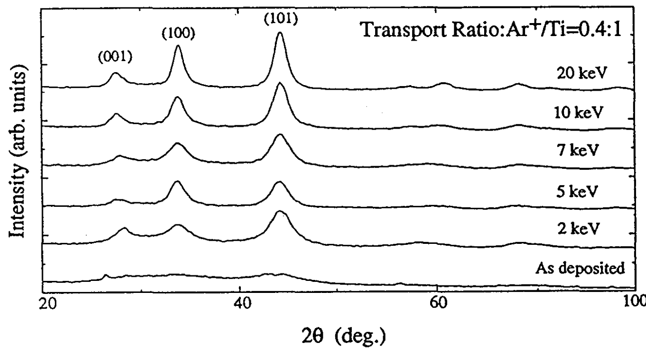

Fig.2 The XRD patterns of IBAD TiB_2 films obtained by glancing angle diffraction

Table 1 The grain size of TiB_2 films as a function of bombarding energy

Sample	Φ (deg.)	φ (rad.)	D (Å)
As deposited	6.9069	0.1204	12
2 keV	2.8084	0.0488	31
5 keV	2.0821	0.0360	42
7 keV	2.2669	0.0393	38
10 keV	1.7247	0.0297	50
20 keV	1.4205	0.0243	61

Φ: measured FWHM of the $TiB_2(101)$ peaks
φ: real FWHM of the $TiB_2(101)$ peaks
D: grain size in diameter calculated by Scherrer method

3.2 The film structure

There are no obvious X-ray diffraction peaks in the XRD of the as-deposited film, suggesting that the as-deposited film, prepared without Ar^+ bombardment, had non-crystalline or very poorly crystallized structure. While clear diffraction peaks, corresponding to crystalline structure, can be seen in the XRD of the films deposited with simultaneous Ar^+ bombardment (See Fig.2) showing the formation of crystalline phase. All the diffraction peaks could be attributed only to TiB_2 and are quite broad, indicating very small grain size. Table 1 lists the FWHM of $TiB_2(101)$ peaks and the grain size of the films. The FWHM values were obtained after the smoothing and peak separation using a Rigaku/Dmax XRD data processing software. Although the XRD spectrum of the as-deposited film did not show clear diffraction peaks, it could be analyzed as the overlaps of several broad peaks (See Fig.3). By applying Scherrer's formula, the grain size of the TiB_2 films can be estimated as follows:

$$D=\frac{k\cdot\lambda}{\phi\cdot\cos\theta} \qquad (1)$$

k= 0.9 as a constant
λ=1.5406 Å for Cu Kα radiation
2θ=44.4 ° for the $TiB_2(101)$ peak, and:

$$\phi^2=\Phi^2-\beta^2 \qquad (2)$$

ß: FWHM caused by the measuring system (here, the FWHM of Si(220) diffraction, 0.2853°, was used)

We can clearly find in Fig.2 and Table 1 that the intensity of the main diffraction peaks increases with increasing Ar^+ energy, while the FWHM decreases. This suggested that TiB_2 films became better crystallized with the increasing amount of energy transferred to the growing film by Ar^+ bombardment, which was one of the key parameters to determine the formation as well as the structure of the crystalline phase in the film prepared by IBAD.

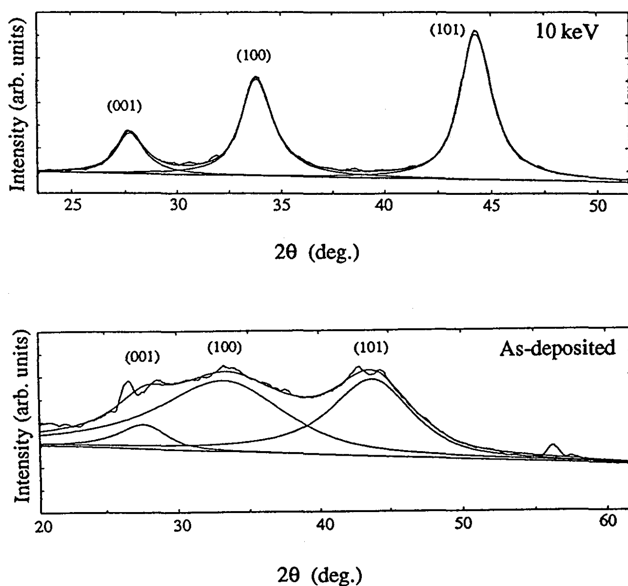

Fig.3 Multi-peak seperation of the XRD patterns of both as-deposited and 10 keV Ar^+ bombarded TiB_2 films

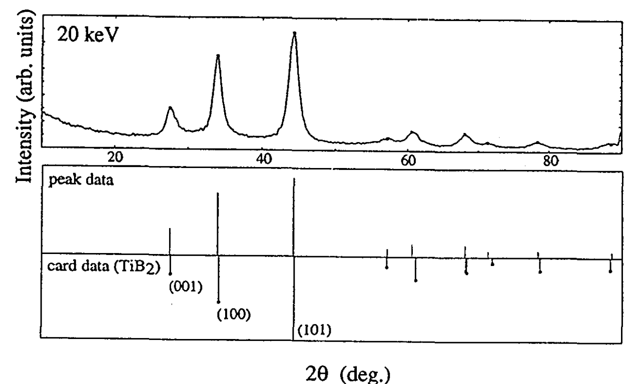

Fig.4 Acomparison between IBAD film and standard XRD data of TiB_2

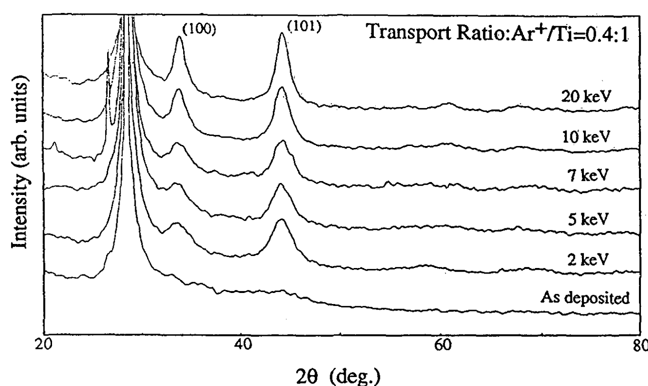

Fig.5 The XRD patterns of IBAD TiB_2 films obtained by standard θ–2θ scanning diffraction

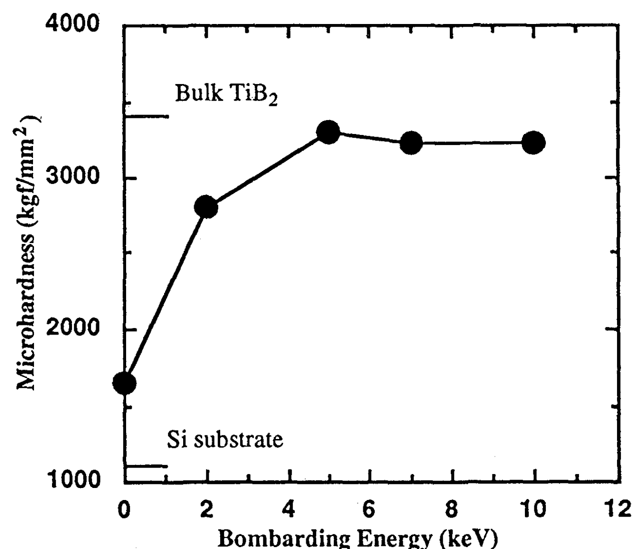

Fig.6 The microhardness of IBAD TiB_2 films as a function of Ar^+ energy

As shown in Fig.4, most of the diffraction peaks of TiB_2 films have a little shift towards the lower angle as compared with the standard data listed in the ASTM card. From peak position, the lattice constants of TiB_2 films are calculated as a=3.0393 Å and c=3.2384 Å, both 0.3% larger than the standard value of TiB_2, indicating an overall expansion of TiB_2 lattice. This might be caused by the presence of interstitial Ar atoms in the TiB_2 lattice.

The preferential orientation has been observed for most of IBAD films. But in this experiment, no preferential orientation of the crystalline TiB_2 films could be observed in the standard θ–2θ XRD data (See Fig.5). Though the mechanism of the preferential growth in IBAD films differs from system to system and is not thoroughly understood, the anisotropic defect production by ion bombardment is believed to play an important role[13,14]. In the IBAD process, some specific lattice plane, most commonly the closest packed plane, would be more seriously damaged by ion bombardment[15]. So the growth in the direction perpendicular to these planes will be eliminated by ion bombardment during the deposition and may result in a preferential orientation. However, in the case of IBAD TiB_2 films, the inter atomic distance in <001>, <100> and <101> direction has a much smaller difference as compared with FCC TiN. This is considered to be one of the factors responsible for the absence of preferential orientation for the films prepared in our study.

3.3 Microhardness of the films

The microhardness of the TiB_2 films was measured using a tester equipped with a Vickers diamond pyramid as an indenter. Several indentations were made with different loads for each sample. Because of the very small film thickness, the minimum load as low as 1 gf was applied in order to eliminate the influence of the substrate hardness. The diagonal of the indentation was measured using both optical microscope and scanning electron microscope (SEM). The measured results of microhardness are shown in Fig.6.

The non-crystalline as-deposited film has the lowest microhardness value of about 1830 kgf/mm^2, while the films deposited with the simultaneous Ar^+ bombardment, with the formation of crystalline TiB_2 phase, has a much higher microhardness. The highest value of microhardness obtained for the film deposited with 10 keV Ar^+ bombardment is about 3340 kgf/mm^2, comparable to the hardness of the bulk TiB_2 material (about 3370 kgf/mm^2)[2]. This result verifies that crystalline TiB_2 films have much higher microhardness than non-crystalline films[11].

4. Conclusion

In our present work, crystalline hexagonal TiB_2 films with stoichiometric composition of 2:1 for B to Ti atomic ratio were obtained using IBAD. The structural characterization by XRD has shown that the films were composed merely of crystalline TiB_2 and no preferential orientation of the films was observed. High energy Ar^+ bombardment has resulted in better crystallization of TiB_2 films due to higher energy deposition to the films. The crystalline TiB_2 films have shown higher microhardness than the non-crystalline as-deposited film and have a value comparable to the bulk TiB_2 material.

Acknowledgment

Great acknowledgment is due to Dr. Y. Makino, and Dr. G. Fujinawa and Mr. Y. Maki of Rigaku Corporation for their great helps in the XRD analysis. The Japan Society for the Promotion of Science has supported this study by awarding a postdoctoral research fellowship to one of the authors.

References

1) A. Kluge, B.H-S. Javadi, H. Ruoff, R. Oechsner and H. Ryssel, Surface and Coating Technol. 51 (1992) 237
2) P.A. Dearnley and T. Bell, Surf. Engineering, 1 (1985) 203
3) G.V. Smsonov and B.A. Kovenskaya, in I. Matkovich (eds.),"*Borone and Refractory Borides*", (Springer-Verlag, Berlin, 1977) 19
4) J.G. Ryan, S. Roberts, G.J. Slusser and E.D. Adams, Thin Solid Films, 153 (1987) 329
5) J. Shappirio, J. Finnegan, R. Lux, D. Fox, and J. Kwiatkowski, J. Vacuum Sci. Technol. A3 (1985) 2255
6) A.J. Becker and J.H. Blanks, Thin Solid Films, 119 (1984) 241
7) C. Mitterer, M. Rauter and P. Rödhammber, Surf. and Coating Technol., 41 (1990) 351
8) E. Broszeit, B. Matthes, W. Herr and K.H Kloos, Surf. and Coating Technol., 58 (1993) 29
9) A.W. Mullendore, D.M. Mattox, J.B. Whitley and D.J. Sharp, Thin Solid Films, 63 (1979) 243
10) J.P Rivière, Ph. Guesdon, G. Farges and D. Degout, Surf. and Coating Technol., 42 (1990) 81
11) J.P Riviѐe, Ph. Guesdon, J. Delafond and M.F. Denanot, Surf. and Coating Technol., 45 (1991) 83
12) Y. Setsuhara, H. Aoki, S. Miyake, A. Chayahara and M. Satou, Nucl. Instrum. and Methods in Phys. Res., B80/81 (1993) 1406
13) M. Kiuchi, A. Chayahara, Y. Horino, K. Fujii, M. Satou, H.J. Kang, Y.W. Beag, Y. Kimura and R. Shimizu, Jpn. J. Appl. Phys., 29 (1990) 2059
14) S. Miyake, T. Kobayashi, M. Satou, F. Fujimoto, J. Vac. Sci. & Technol. 9 (1991) 3036
15) Chr. Lehmann, '*Interaction of Radiation with Solids and Elementary Defect Production*", in S. Amelinkey, R. Gevers and J. Nihoul (eds.), '*Defects in Crystalline Solids*', (North-holland Publishing Company, 1977), p.199